2.6 Machine Detector Interface

2.6.1 Overview

The Machine Detector Interface (MDI) region deals with the part of the CLIC facility within the detector cavern, where there is a strong coupling between technical subsystems of the machine and the physics detectors. An important aspect is the conceptual design, alignment, stabilization and integration of the final focusing quadrupoles, QD0, within the detectors. These quadrupoles play a key role in achieving the nominal vertical beam size of 1 nm r.m.s., necessary to achieve the nominal luminosity at 3 TeV centre-of-mass energy. Any vertical movement of the quadrupole would provoke a displacement of the beam at the interaction point by a comparable amount. To avoid such movements, its vertical position must be stabilized to 0.15 nm at frequencies above 4 Hz. Lower frequencies are mainly compensated by beam-based feedback and feed-forward loops in the linacs and beam delivery systems. Also other systems for luminosity optimization have been introduced, such as intra-pulse feedback, which corrects the beam position within the 156 ns pulse train. It should be noted that vibrations at frequencies close to the machine frequency of 50 Hz and its higher harmonics have a strongly reduced impact on the machine performance.

The spent beams have a power of 14 MW each and must be transported away cleanly through the experiment onto two beam dumps, via the post-collision lines. The beam dumps are located at a distance of 315 m from the interaction point. Backgrounds in the detectors from the dumps, as well as muons from the collimators in the beam delivery system and beam-beam backgrounds, must be minimized. Finally, radiation to detectors and people must be minimized by appropriate shielding and cavern layout.

The detector layouts are based on the ILC detectors SiD [1] and ILD [2], but adapted to the CLIC specific parameters. For both detectors a layout drawing exists with the beam-related elements integrated, including QD0 and related instrumentation. The distance L^* between the exit of the QD0 quadrupole and the interaction point is 3.5 m for the CLIC_SiD detector and 4.34 m for CLIC_ILD. The shorter L^* is considered the most challenging and delivers in principle the higher luminosity, therefore we have mostly concentrated on this layout in the present document. The final L^* value, and the option of having two different L^* values for the different detectors, will be addressed at the Technical Design Report stage.

For the CLIC_SiD option, the required gradient of the QD0 magnet is 575 T/m. Some tunability of the gradient is required to allow energy scans over a limited range, from nominal to 20%-below nominal.

As, according to measurements around the CMS detector [3], the ground motions and technical noise are much larger on the detector (as much as 80 nm on top of the yoke) than at the ends of the tunnel (few nanometres), it was decided to support the QD0 magnet from a very stiff support, attached to the tunnel floor via a high-mass pre-isolation system exhibiting a very low natural frequency. Active stabilization of the quadrupole will then be achieved with different gauges and piezo-actuators.

Provisions are made for having two detectors running alternately, each one being installed on a push-pull platform. Once installed on the beamline access to the inner detector will not be possible and a move to the garage position will be required for this purpose. During the detector movement the QD0 magnets will be supported from the detector. Once in the garage position they can be removed from the detector to allow a full opening.

A simplified view of the Machine Detector Interface is shown in Figure 1. Technical details will be described in Chapter 5.

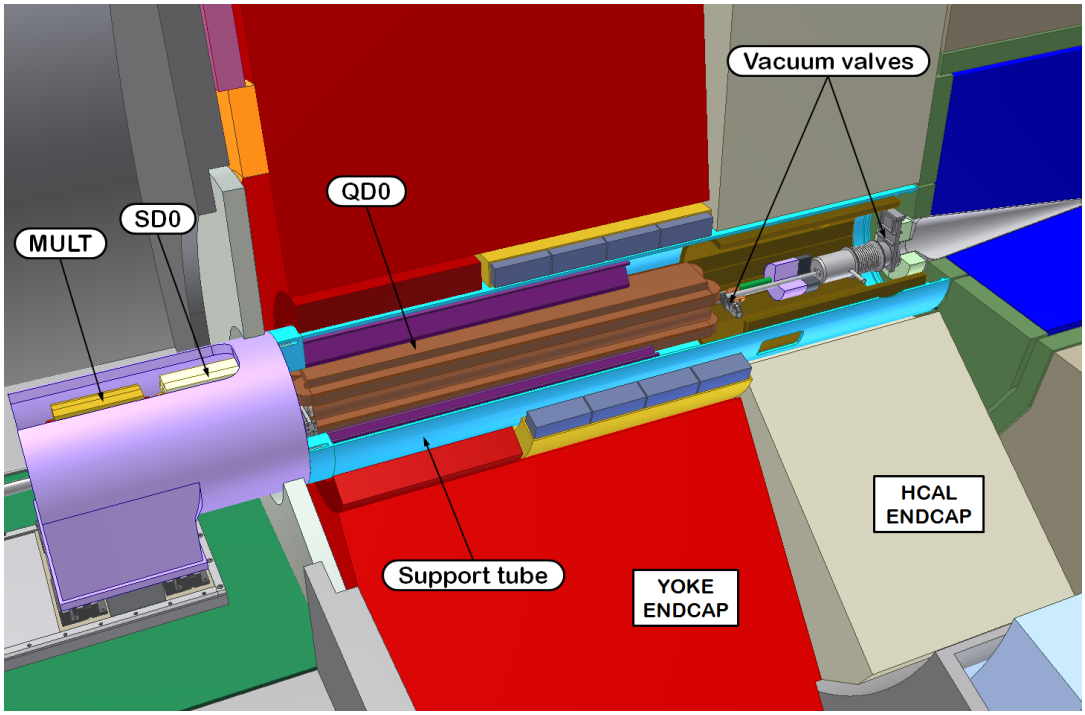

Fig.1: MDI layout view (simplified). It shows in particular a representation of part of the final focus quadrupole QD0, integrated in the CLIC_SiD detector.

2.6.2 Beam parameters

Nominal values of the beam parameters of interest for the Machine Detector Interface are listed in Table 2.1. Among the more relevant parameters are the vertical beam spot size at the interaction point and the length of the bunch train.

Table 2.1: The beam parameters that are of interest to the MDI region

Beam parameter	Value
Centre of mass energy	3 TeV
Total Luminosity	$5.9\ 10^{34}$ cm^{-2}s^{-1}
Luminosity L_{99} (within 1% of energy)	$2\ 10^{34}$ cm^{-2}s^{-1}
Linac repetition rate	50 Hz
Number of bunches per train	312
Number of particles per bunch	$3.72\ 10^{9}$
Bunch separation	0.5 ns
Bunch train length	156 ns
Beam power per beam	14 MW
Nominal horizontal IP β function	6.9 mm
Nominal vertical IP β function	0.068 mm
Horizontal IP beam size	45 nm
Vertical IP beam size	1 nm
Bunch length	44 μm

2.6.3 System descriptions

2.6.3.1 QD0 and support

In Figure 1 some major components of the Machine Detector Interface can be identified, including the QD0 quadrupole. The tight integration of the QD0 magnet itself, including the vacuum pipe of the incoming beam (smaller diameter) and the vacuum pipe of the outgoing beam (bigger diameter), should be noted.

The incoming and outgoing beam lines cross at an angle of 20 mrad (the beam crossing angle) and the outgoing (post-collision) vacuum pipe will have a conical shape with a half opening angle of 10 mrad.

A major consequence of these geometrical considerations is that the post-collision vacuum pipe must be housed inside the QD0 and subsequent magnets until the point where the separation of the two vacuum pipes is sufficient to allow a change to a different magnet cross section with the post-collision line running externally to the magnets.

2.6.3.1.1 QD0 Main Parameters

The design parameters for the QD0 quadrupole [4] are defined by the Beam Delivery System and listed in Table 2.2:

Table 2.2: QD0 main parameters

Parameter	**value**
Magnet Aperture (diameter)	8.00 mm
Nominal Gradient	575 T/m
Effective length (magnetic)	2.73 m
Required tunability of the Gradient	80-100 %

2.6.3.1.2 Technical Design Choice

We have investigated the concept of a compact "hybrid" magnet working with a permanent magnet (PM) and classical electro-magnetic (EM) coils, rather than using super-conducting technology (see Section 5.10.2.1 for details of the magnet design). The main reasons are:

- the space available around the magnet is extremely limited, therefore it is not easy to assemble and integrate a cryostat with all the ancillary components and systems,
- the magnet aperture is very small, and it will be difficult to precisely wind superconducting cables in a sound design within the available space so as to withstand the huge electromagnetic forces on so small radius,
- the difficulties to actively align and stabilize, at the sub-nanometer level, the complex assembly of a superconducting magnet, containing the different layers of coils, collars or other force-bearing structures, thermal insulation, thin supports, cryostat, etc.,
- the difficulty to design a cryostat assembly allowing the integration of a conical post-collision line,
- the extreme level of stability required at the IP due to the small beam size, combined with the limitations of the IP feedback system due to its latency and the specific CLIC time structure, makes the use of superconducting technology difficult to apply.

For CLIC the alternative solution of using a permanent-magnet-based QD0 quadrupole seems to satisfy all requirements.

2.6.3.1.3 QD0 Support

Figure 2 shows again a conceptual layout of the MDI region and in particular how several elements, namely QD0, BeamCal, LumiCal and the feedback kicker, will be supported by two tubes that will be cantilevered from the cavern wall. Details of this removable support tube, which is a key element of the "push-pull", stabilization and alignment systems, are presented in Section 5.10.2.5.

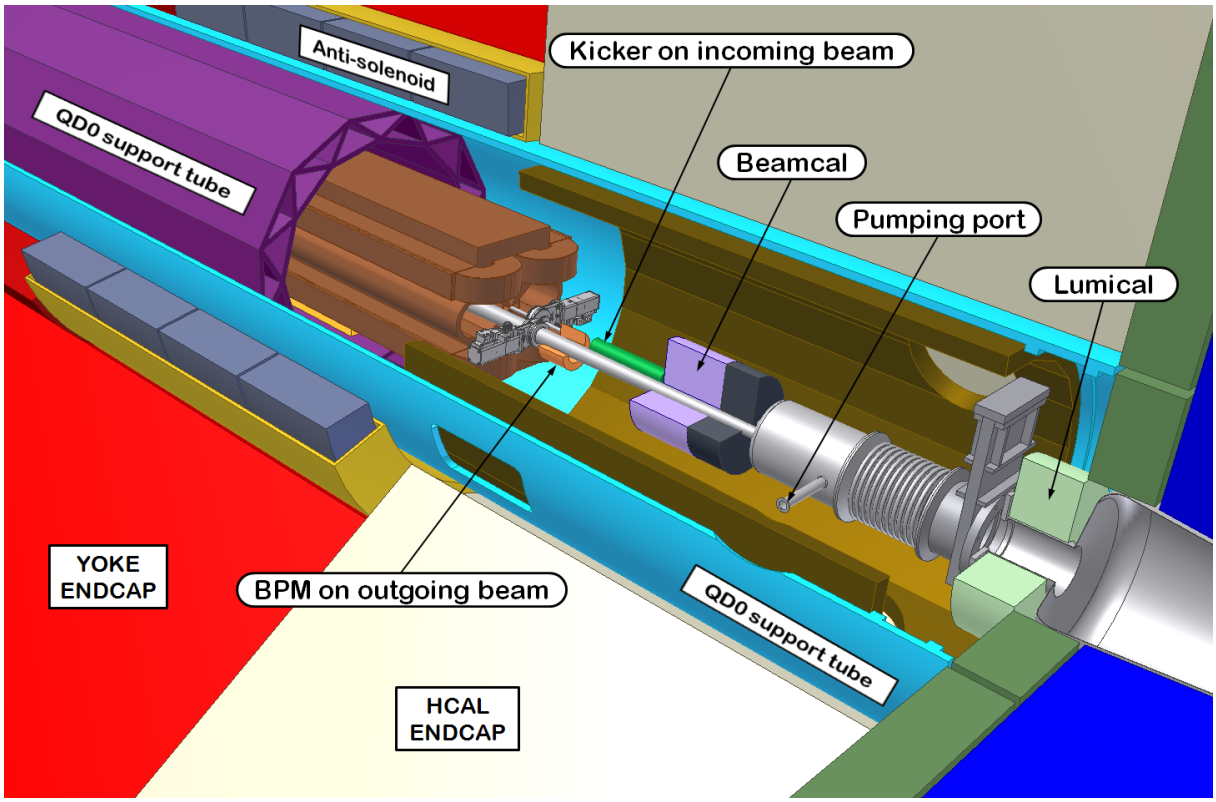

Fig. 2: Support tube concept in the MDI region

2.6.3.2 Anti-solenoid

Due to the crossing angle, the magnetic field of the main detector solenoid [5] exhibits a component perpendicular to the incoming beams. This leads to several distortions of the beam at the IP as described in [4,5]. The most severe effects originate from the overlap between the main solenoid and QD0 fields [6-9]. Due to the short L* values the main detector solenoid and the QD0 fields interfere. In addition since permendur and permanent magnet material are considered in the QD0 design [10], the shielding of QD0 from the external field is necessary. In order to achieve both the shielding of the QD0 magnet and the reduction of the beam distortions, an anti-solenoid has been proposed [11]. Preliminary designs of such an anti-solenoid consist presently of bucking coils surrounding the QD0 support tube and connected to the detector end-caps. The current of each bucking coil is adjusted in order to minimize the detector solenoid flux density along the beam trajectory. Beam dynamics simulations show that it cancels more than 90% of the beam distortions at the IP [8]. The simulated field map is shown in Figure 3 for the CLIC_SiD case.

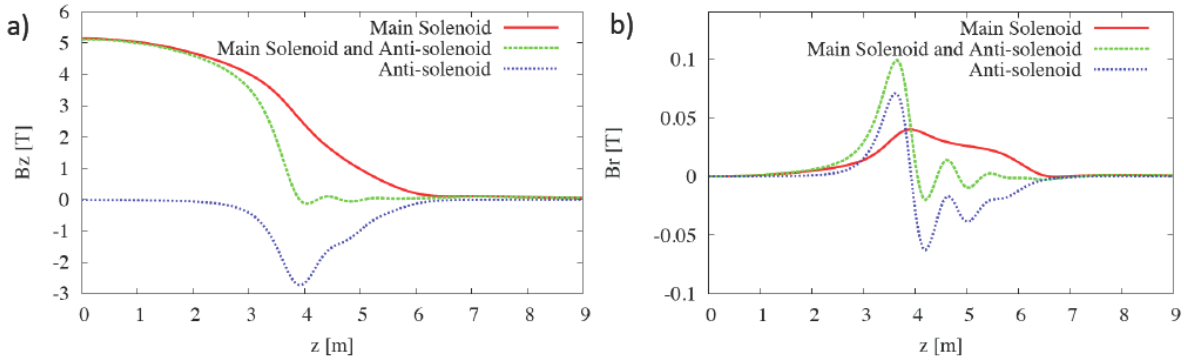

Fig. 3: The longitudinal field after compensation with the anti-solenoid is shown in (a), the radial field in (b), for the CLIC_SiD layout

The anti-solenoid also reduces the effect of the main solenoid on the luminosity. Already in the present (not yet optimized) design, the remaining luminosity reduction is only half of the total BDS budget for luminosity loss.

In the L^* = 6 m option (a backup solution where the QD0 is mounted outside the detector, in the tunnel, but with reduced luminosity) the anti-solenoid would be simpler: the bucking coils can have a smaller radius and just surround the QD0 magnet. Further optimization of the bucking coils design and the overall integration of the anti-solenoid within the MDI region are foreseen for the TDR phase.

2.6.3.3 Forward region design

Figures 1 and 2 show the current design of the forward region for one of the detector concepts envisaged, the CLIC_SiD detector. The forward region contains two forward detectors that complete the coverage for small angles. The Luminosity Calorimeter (LumiCal) [12] for precision luminosity measurements and an instrumented absorber for beam-beam background pairs (BeamCal) and for high energy electron tagging. Together they complete the angular coverage down to a polar angle of 11 mrad. Since the BeamCal is located closest to the beams, it also acts as a mask against particles back-scattering from the beam dump.

The LumiCal is an electromagnetic sandwich calorimeter consisting of 40 layers of 3.5 mm tungsten absorbers with silicon sensors, covering an angular region from 40 to 110 mrad. It is designed to count Bhabha events and gives a slow but precise measurement of the luminosity. The goal for the luminosity precision is 1% for an integrated luminosity of 100 fb^{-1}. The lower acceptance angle of the LumiCal is chosen to reduce the number of incoherent pairs that hit it. These could otherwise reduce its energy resolution.

The BeamCal is another electromagnetic sandwich calorimeter, consisting of 40 layers of 3.5 mm tungsten absorbers and sensors. To reduce back-scattering from the surface of the BeamCal a 10 cm thick graphite disk is placed on the IP-facing side. Because of the large radiation dose of up to several MegaGray per year, a radiation-hard sensor material has to be used. The BeamCal extends the angular coverage down to 11 mrad and is therefore the primary absorber of background pairs that might otherwise damage the final focus quadrupole or the equipment of the intra-train feedback system. At the ILC the BeamCal will be used for the tagging of high-energy electrons, and the distribution of deposited energy from the background pairs can also be used for beam diagnostics [13]. It remains to be confirmed whether these applications are also possible at CLIC.

2.6.3.4 Intra-train feedback system

A fast beam-based intra-train feedback (FB) system is foreseen to correct for the relative vertical displacement of the colliding beams at the IP by steering them back into collision. This FB system can be considered as the last line of defense against relative beam-beam offsets, and it may also help to relax the tight vibration tolerance of the QD0 quadrupoles. At CLIC intra-train FB is especially challenging due to the extremely small bunch separation of 0.5 ns and bunch train length of 156 ns. With current technology one cannot apply bunch-to-bunch corrections, but can only make a few correction iterations per train by using an all-analogue FB system. No intra-train angle FB system is currently planned due to latency time constraints.

The key components are a beam position monitor (BPM) based on stripline pickups for registering the position (and hence deflection angle) of the outgoing beam; a front-end signal processor and feedback circuit; an amplifier to provide the required output drive signals; and a kicker for applying an angular correction to the opposite incoming beam. The BPM and kicker locations are shown in Figure 2.

Such a system would be deployed (to provide backup) on both sides of the IP. Details of prototype components and system tests with real beams are given in [14]. For this layout the total latency, due to beam time of flight and hardware delays, can be kept to 37 ns or less [15]. This allows for approximately three luminosity correction cycles during the bunch train duration, as shown in Figure 4. This example corresponds to a simulation based on a single random seed of (very noisy) ground motion for the element misalignments in the BDS, and considers a perfect linac. A detailed description of the potential luminosity recovery performance is given in [15].

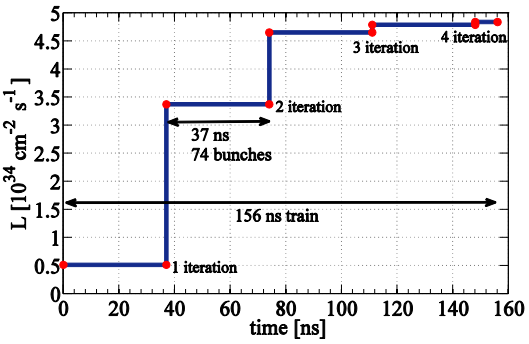

Fig. 4: Simulated luminosity versus bunch number for nominal CLIC 3 TeV parameters and assuming a noisy site for the ground motion.

2.6.3.5 Vacuum system

Conceptually the MDI vacuum system is composed of three physically connected sectors (QD0, experimental and post-collision lines) with different requirements.

The QD0 sector consists of an incoming beam chamber inside the magnet and a post-collision chamber passing through the magnet structure. CLIC plans to use room temperature QD0 magnets as opposed to the superconducting QD0 planned for the ILC. This means that the CLIC QD0 will not be able to profit from the high capacity cryo-pumping available within a magnet cold bore. However, simulations for CLIC [16] and ILC [17] show that incoherent instabilities and beam gas background are acceptable in this region up to pressures of 10^5 nTorr and 10^3 nTorr respectively. These relatively relaxed pressure requirements suggest that local lumped pumping from the extremities of the magnet may be feasible.

An additional constraint is imposed by the detector push-pull concept, which implies by definition that the beam vacuum must be separated to switch detectors. The system must therefore be designed so that the required operating pressure can be obtained within ~24h of re-connecting the push-pull sector.

The experimental vacuum sector must combine BDS vacuum requirements with the needs of the surrounding detectors. CLIC detectors have requested a geometry consisting of a cylindrical section inside the vertex detector with symmetric cones on either side. The vacuum system design (chambers, supports, instrumentation) within each detector must be optimized to present the minimum radiation length within the detector acceptance. Low-Z materials such as beryllium and aluminium also have high secondary emission yields. Optimizing the vacuum chamber for physics may therefore imply the use of coatings and/or in-situ heating of the chamber to maintain vacuum stability.

The post-collision line vacuum has a less demanding pressure requirement in the medium vacuum range, allowing for a conventional un-baked system design.

2.6.4 Accelerators Physics issues

Luminosity spectrum and accelerator background levels strongly influence the experimental conditions and have an important impact on the detector design. Two main sources of background can be identified: those coming from the beam interactions before and after the collision point, the so called machine backgrounds, and those arising from beam-beam effects, the so called beam-beam background.

2.6.4.1 Luminosity spectrum

Figure 5 shows the total luminosity spectrum and the luminosity in the peak for the CLIC nominal beam parameters listed in Table 2.1. The small transverse dimensions at the collision point combined with high energies lead to strong beam-beam effects (beamstrahlung mainly), which smear the luminosity spectrum. The single-bunch energy spread (due to the RF structures) has been optimized to minimize their contribution as much as possible. Coherent processes (see next section) also contribute to luminosity (~4%) increasing mainly the low-energy tail of the spectrum. They create collisions where an electron, from a coherent pair produced in the positron beam, collides with the electron beam (and vice versa). The contribution of these collisions to the luminosity spectrum (~1%) is shown in red in Figure 5.

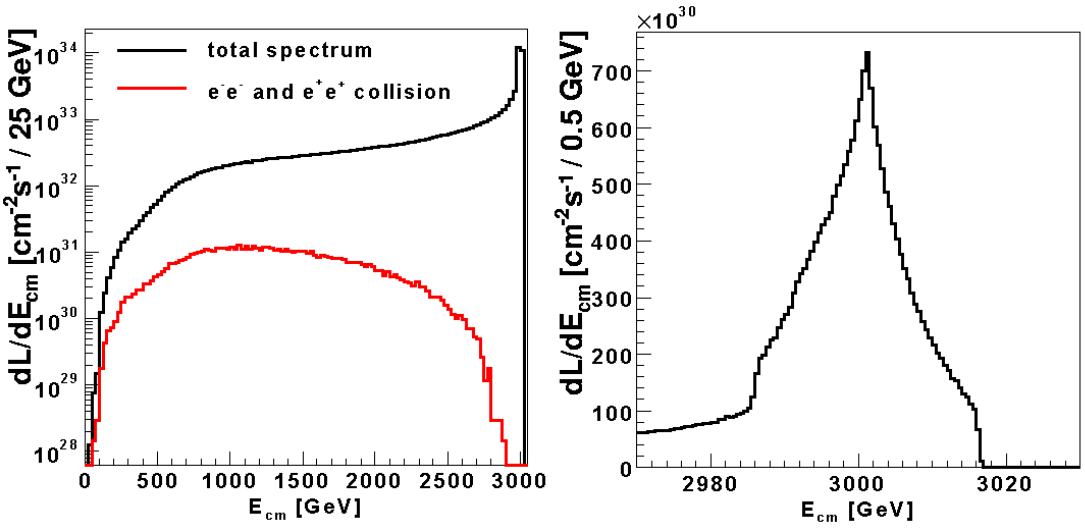

Fig. 5: Total luminosity spectrum (left) and zoomed view of the luminosity in the peak (right).

2.6.4.2 Beam-Beam background

In order to achieve the required luminosity the beams are focused to very small sizes. In electron-positron collisions the electromagnetic field of each bunch will focus the other, leading to an enhancement of luminosity. Due to the strong bending of their trajectory, the beam particles will emit high-energy photons, so-called beamstrahlung. In addition to beamstrahlung photons QED and QCD backgrounds are produced during collisions. The relevant processes are: coherent pair production, incoherent pair production and $\gamma\gamma \rightarrow$ hadrons events. At the CLIC energy higher order coherent processes also have a significant production rate, the so-called tridents [18]. A detailed description of the production processes and typical cross-sections can be found in [19]. The expected rates per bunch crossing for the nominal CLIC parameters of Table 2.1 are reported in Table 2.3.

During operation the luminosity can be higher than its nominal value, as the nominal emittance is smaller than the acceptance. This causes the background levels to increase to up to 40% higher than nominal. Imperfections will in turn lead to a reduction of the luminosity with respect to this increased level. They will also result in reduced background levels, but the ratio of background to luminosity may nevertheless increase [20].

Table 2.3: Expected background rates for the CLIC nominal beam parameters.

Background	**Rate per bunch crossing**
Beamstrahlung photons	2.1 per primary particle
Incoherent pairs	3.3×10^5 particles
Coherent pairs	6.6×10^8 particles
Tridents	6.7×10^8 particles
$\gamma\gamma \rightarrow$ hadrons (> 2 GeV)	3.2 events

2.6.4.3 Machine background

Beam halo particles are stopped by the collimators of the beam delivery system (BDS), but the secondary muons produced in the collimators can reach the detector. The absolute muon flux depends on the number of halo particles that impact on the collimators, which in turn depends on the collimators settings and on details of the lattice, including imperfections and misalignment. Considering only halo particles generated by the beam-gas scattering mechanism, and assuming a perfect BDS lattice, a fraction of $2x10^{-4}$ of the beam is found to hit the spoilers, producing a flux of $1.2x10^4$ muons/train at 10 m from the interaction point within a 6 m radius around the beam line [21]. Muon suppression methods are discussed in section 2.5.3.4.

The disrupted beams after the collision and the pairs produced during the interaction are transported to the main dump with minimal losses. Nevertheless interactions occur in the carbon magnet protection absorbers, at the intermediate dump and at the main dump [22]. These interactions generate backscattered photons and neutrons that can reach the detector. The flux from the intermediate dump through a 2x2 m^2 plane at 0.0 m is calculated as 8.4 ± 2.8 photons per cm^2 per bunch crossing, with an average energy of 162 ± 4 keV. Further details as well as the estimated neutron flux can be found in chapter 2.7.

Typical synchrotron radiation fans from the final doublet (QF1 and QD0) to the interaction region are depicted in Figure 6, for an envelope covering 15 standard deviations in x and 55 in y. At the IP the photon cone is inside a cylinder with radius of 5 mm and thus within the beam pipe radius. Therefore, they will not affect the detectors significantly.

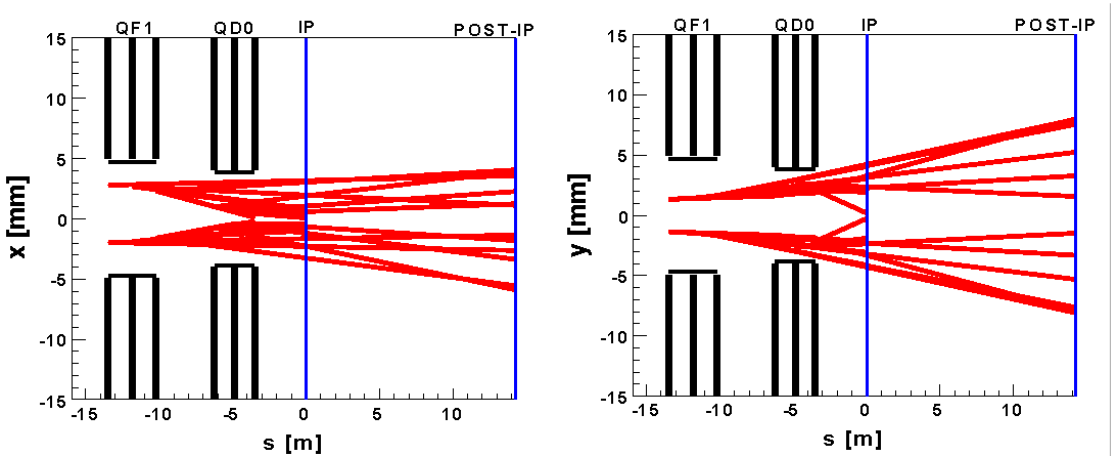

Fig. 6: Synchrotron radiation fans at 3 TeV centre-of-mass energy.

2.6.5 Component specifications

The main components and their required specifications are listed in Table 2.4.

Table 2.4: Specifications for the main components in the Machine Detector Interface region

Component	Number	Requirements
QD0 magnets	4	Gradient 575 T/m, length 2.73 m, aperture radius 3.8 mm
QD0 stabilisation systems	2	R.M.S. movements < 0.15 nm above 4 Hz, in combination with diverse feedback systems
QD0 Prealignment systems	2	Alignment precision 10 μm
Vacuum system		10^3 nTorr in MDI region
IP feedback system	4	37 ns latency (1/4 of train length)
Anti-solenoids	4	Solenoid cancellation to below 0.2 T

References

[1] H. Aihara, P.N. Burrows, M. Oreglia (Eds.) et al., SiD Letter of Intent, 2009.

[2] ILD Concept Group, The International Large Detector Letter of Intent, 2009, DESY 09-087.

[3] K.Artoos et al., Proceedings of PAC09, Vancouver BC, Canada, TH5RFP081, EUCARD-CON-20090021, http://cdsweb.cern.ch/record/1239667.

[4] R.Tomás, Technical specifications of the CLIC Final Doublet quadrupoles, EDMS #976036.

[5] See Vol. III, chapter 9, section 2.

[6] Y. Nosochkov and A. Seryi, Phys. Rev. Spec. Top-Acc. and Beams 8, 021001 (2005).

[7] B. Dalena, D. Schulte, R.Tomás and D. Angal-Kalinin TH6PFP074, PAC09 proceedings and CLIC-Note-786.

[8] B. Dalena, D. Schulte and R. Tomás WEPE029, IPAC10 proceedings and CLIC-Note-831.

[9] J.J. Murray, SLAC-CN-237.

[10] See section 2.6.3.1.2.

[11] D. Swoboda, B. Dalena and R. Tomás, "CLIC spectrometer magnet interference computation of transversal B-field on primary beam", CERN-OPEN-2010-016 and CLIC-Note-815.

[12] I.Sadeh, H.Abramowicz, R.Ingbir, S.Kananov and A.Levy, A Luminosity Calorimeter for CLIC, LCD-Note-2009-002, 2009.

[13] Ch.Grah and A.Sapronov, JINST 3 P10004 (2008).

[14] P.N. Burrows et al., 'Tests of the FONT3 Linear Collider Intra-train Beam Feedback System at the ATF', Proceedings PAC05, Knoxville, TN, May 2005, p. 1359.
P.N. Burrows et al.,'Performance of the FONT3 fast analogue intra-train beam-based feedback system at ATF'; Proceedings EPAC06, Edinburgh, UK, June 2006, p. 852.

[15] J. Resta-Lopez, P.N. Burrows and G. Christian: 'Luminosity Performance Studies of the Compact Linear Collider with Intra-train Feedback System at the Interaction Point', JINST5, P09007 (2010)

[16] G.Rumolo, private communication, see also http://indico.cern.ch/getFile.py/access?contribId=1&resId=0&materialId=slides&confId=86050

[17] T.Maruyama, LCWA 2009, Albuquerque

[18] J. Esberg et al., to be published

[19] D. Schulte, " Study of electromagnetic and hadronic background in the interaction region of the TESLA collider", PhD thesis, TESLA 97-08 (1996).

[20] B. Dalena and D. Schulte, "Beam-beam background in CLIC in presence of imperfections" WEPE025, proceeding of IPAC'10

[21] H. Burkhardt et al., "Muon Background in CLIC", THPD014, proceeding of IPAC'10

[22] M. Salt et al., " *Background at the Interaction Point from the CLIC Post-Collision Line*", CLIC-Note-847